

Nernst Effect in Electron-Doped $\text{Pr}_{2-x}\text{Ce}_x\text{CuO}_4$

Hamza Balci, C.P.Hill, M. M. Qazilbash, and R. L. Greene

Center for Superconductivity Research, Department of Physics, University of Maryland,

College Park, MD-20742

(March 1, 2019)

Abstract

The Nernst effect of $\text{Pr}_{2-x}\text{Ce}_x\text{CuO}_4$ ($x=0.13, 0.15,$ and 0.17) has been measured on thin film samples between 5-120 K and 0-14 T. In comparison to recent measurements on hole-doped cuprates that showed an anomalously large Nernst effect above the resistive T_c and H_{c2} [1–4], we find a normal Nernst effect above T_c and H_{c2} for all dopings. The $H_{c2}(T)$ determined from the Nernst effect shows a conventional behavior for all dopings. The energy gap determined from $H_{c2}(0)$ decreases as the system goes from under-doping to over-doping. The contrasting behavior of the Nernst effect above T_c in hole and electron-doped cuprates suggests that conventional superconducting fluctuations are the cause of the large signal in the hole-doped compounds.

PACS no.s: 74.25.Fy, 74.40.+k, 74.72.Jt

Introduction

Recent Nernst effect measurements [1–4] on hole-doped cuprate high- T_c superconductors have shown very surprising results. Especially in the under-doped regime of these cuprates, an anomalous Nernst signal has been observed to persist to temperatures up to 50-100 K above T_c , and to magnetic fields much larger than the resistive H_{c2} . The authors have interpreted this anomalous signal above the conventional T_c or H_{c2} (the T_c or H_{c2} of resistivity and magnetization) as evidence for vortex like excitations, and have defined a new T_c and H_{c2} for these compounds. In their picture there is a temperature (or field) at which the Cooper pairs start to form, and another temperature(or field) below which the Cooper pairs attain phase coherence throughout the sample. In this picture the T_c (or H_{c2}) of resistivity measurements corresponds to the temperature (or field) that coherence has been obtained, whereas the onset of the anomalous Nernst signal corresponds to the temperature (or field) of the Cooper pair formation. The authors also suggest that this anomalous Nernst signal is related to the pseudogap or some interaction between the pseudogap state and the superconducting state since the Nernst signal follows a pattern similar to the pseudogap phase diagram(i.e. the signal above T_c is more pronounced in the under-doped regime) [5].

These Nernst effect measurements have inspired a revisit to the theory of superconducting fluctuations in the cuprates. These theoretical studies have proposed that the anomalous Nernst effect can be explained without assuming vortex-like excitations. Kontani suggests that including antiferromagnetic fluctuations in addition to superconducting fluctuations in the under-doped regime would explain the unusually large Nernst signal above T_c [6]. Usishkin *et al.* [7] suggest that Gaussian superconducting fluctuations above T_c are able to explain the Nernst effect for the optimally-doped and over-doped regimes. For the under-doped regime they suggest that strong non-Gaussian fluctuations reduce the mean-field transition temperature T_c^{MF} and therefore the mean field T_c^{MF} should be used in calculations instead of the actual T_c in order to take into account the contribution of the non-Gaussian fluctuations to the Nernst effect [7]. Another proposal came from Tan *et al.* [8] in which they proposed a preformed pair alternative to the vortex-like excitations scenario to explain

the anomalous Nernst effect in the under-doped hole-doped cuprates. At present, none of the proposed explanations (vortex-like excitations above T_c , strong superconducting fluctuations, or pseudogap) for the large Nernst signal observed in the hole-doped compounds have gained general acceptance.

Early measurements on hole-doped cuprates, which were concentrated on the optimally-doped regime, showed a large Nernst signal below T_c (the well known vortex Nernst effect) which diminished rapidly close to T_c (H_{c2}), and merged to the normal state Nernst signal [9]. This behavior was similar to that observed in conventional superconductors, except for a broader fluctuation regime. The Nernst effect studies in the electron-doped cuprate superconductors (all previous measurements were on $\text{Nd}_{1.85}\text{Ce}_{0.15}\text{CuO}_{4-\delta}$ (NCCO)) showed the same behavior in the superconducting state. However, the normal state behavior was quite different [10–12]. The anomalously large Nernst voltage in the normal state was interpreted as evidence for the existence of two types of carriers, not vortex-like excitations. The two carrier interpretation has recently been supported for optimal doping by ARPES measurements which showed electron pockets on a hole-like Fermi surface [13]. The doping dependence of the Nernst effect in the electron doped superconductors was studied by varying the oxygen content of NCCO, but the cerium doping dependence was not investigated.

In this paper we report Nernst effect data for the electron-doped superconductor $\text{Pr}_{2-x}\text{Ce}_x\text{CuO}_4$ (PCCO) at different cerium dopings, and discuss some of the important issues that were raised by the recent Nernst effect measurements on the hole-doped compounds. Magnetic field and temperature dependence of the Nernst voltage, and temperature dependence of H_{c2} close to T_c are presented. In addition, H_{c2} values obtained from Nernst effect and resistivity are compared. Unlike the hole-doped compounds, our data does not show an anomalous Nernst signal above T_c (or H_{c2}) for the optimally-doped and over-doped compounds. However, the under-doped compound shows a larger fluctuation regime. The $H_{c2}(T)$ obtained from Nernst effect follows a conventional linear temperature dependence close to T_c for all dopings we studied in contrast to an anomalous curvature found in many previous resistivity determinations of $H_{c2}(T)$. $H_{c2}(0)$ and the superconducting energy gap

deduced from $H_{c2}(0)$ increase with decreasing doping even though T_c has a different doping dependence. The magnitude of the Nernst signal in the normal state is very similar for different cerium dopings. It is too large to be explained by a one carrier (one-band) model and it does not show the temperature dependence to be caused by vortex-like excitations or superconducting fluctuations. This suggests that two types of carriers (bands) exist in all the cerium dopings we studied and they are the origin of the large Nernst signal above T_c .

Theoretical Background

The Nernst effect is a thermomagnetic effect, in which a transverse potential difference is induced in the presence of a longitudinal thermal gradient and a perpendicular magnetic field. In a normal metal carriers moving along a thermal gradient accumulate on the cold side of the sample and they induce an electric field opposing the thermal force. This electric field in turn induces an electric current in the opposite direction to the thermal current. In steady state these two currents are equal in magnitude and opposite in sign, so that $J_x=0$ (assuming the thermal gradient is in the \hat{x} direction). In the presence of a magnetic field along \hat{z} direction, the carriers moving in $+\hat{x}$ and $-\hat{x}$ directions will be deflected to opposite sides along the y-axis. In the simplest case of a spherical Fermi surface and one type of carrier, these two currents will be equal to each other, and no transverse voltage will be induced. However in general the two currents will not cancel out exactly because of the energy dependence of the scattering time [14]. In order to satisfy the boundary condition of $J_y=0$, a transverse potential has to be induced, which is the Nernst voltage.

Following Ref [2] we can summarize these ideas by starting from the general equation:

$$\mathbf{J} = \bar{\sigma} \cdot \mathbf{E} + \bar{\alpha} \cdot (-\nabla T) \quad (1)$$

where $\bar{\sigma}$ is the electrical conductivity tensor and $\bar{\alpha}$ is the thermoelectric (Peltier) tensor. Solving Eq.1 for J_x yields:

$$J_x = \sigma_{xx} E_x + \alpha_{xx} (-\partial_x T). \quad (2)$$

The first term in Eq.2 is the current due to the electrical potential of the accumulating

charge on the cold side of the sample, and the second term is the thermal current due to the applied temperature gradient. Imposing the boundary condition $J_x = 0$ on Eq.2 results in:

$$E_x = \frac{\alpha_{xx}\partial_x T}{\sigma_{xx}}. \quad (3)$$

Solving Eq.1 for J_y yields:

$$J_y = \alpha_{yx}(-\partial_x T) + \sigma_{yx}E_x + \sigma_{xx}E_y + \alpha_{yy}(-\partial_y T). \quad (4)$$

The first two terms in Eq.4 are due to deflection of the carriers moving in the $\pm\hat{x}$ directions(the two terms in Eq.2) by the magnetic field in the \hat{z} direction, the third term is the required Nernst effect to satisfy the boundary condition of $J_y=0$, and the fourth term is due to the temperature gradient along y-axis(Righi-Leduc effect). The Righi-Leduc effect can be ignored for thin film samples since the substrate with its large phonon thermal conductivity acts as a shorting medium and prevents a transverse temperature gradient to be established. In measurements on crystals this term can not usually be ignored and it complicates the unambiguous determination of the Nernst signal. By using Eq.3 and Eq.4 (after ignoring the last term), the condition $J_y=0$, and the definition $e_y = E_y/|\partial_x T|$ (the Nernst voltage per unit temperature gradient), the equation:

$$e_y = (\alpha_{yx}/\sigma_{xx}) + (\sigma_{yx}/\sigma_{xx})E_x = [\alpha_{yx}/\sigma_{xx} - S \tan \theta] \quad (5)$$

can be obtained. The last equation results from substituting in the tangent of the Hall angle $\tan \theta = \sigma_{yx}/\sigma_{xx}$, and thermopower $S = \alpha_{xx}/\sigma_{xx}$. Due to the linear magnetic field dependence of E_y (Lorentz force), the Nernst signal should have a linear magnetic field dependence for a normal metal.

The two terms on the RHS of Eq.5 cancel exactly for a normal metal with only one-type of carrier and with an energy independent scattering time (τ). This has been called "Sondheimer cancellation" in the papers of Ong and coworkers [1]. Even with an energy dependent τ in a one-carrier system e_y is very small. In contrast, in a two-carrier system the signal will depend on the thermoelectric and electric conductivities of both bands, and

e_y in this case can be large (see Ref. [11]). This is the argument that was invoked previously to explain the large Nernst signal found in the normal state of the n-doped NCCO [10–12].

For superconductors the thermomagnetic effects have a different mechanism. In the Meissner state the superconducting condensate has a uniform entropy, and there are no single charge carriers like electrons or holes. Therefore, applying a thermal gradient does not induce any flow. In the mixed state there are vortices that carry additional entropy compared to the superconducting condensate around them. Vortices experience a pinning force, f_p , which prevents them from flowing. In the case of an applied thermal gradient, the vortices carrying a transport entropy per unit length of S_ϕ experience a thermal force per unit length of:

$$\mathbf{f}_{\text{th}} = -\mathbf{S}_\phi \nabla T \quad (6)$$

When the thermal gradient and the magnetic field are large enough for thermal force to overcome the pinning force, a viscous flow of vortices is observed. This flow can be represented by:

$$\eta \mathbf{v}_\phi = -(\mathbf{f}_p + \mathbf{S}_\phi \nabla T) \quad (7)$$

where η is the damping coefficient, and \mathbf{v}_ϕ is the velocity of vortices. Josephson showed that a vortex moving in a perpendicular magnetic field induces a transverse electric field given by $(\mathbf{E} = -\mathbf{v}_\phi \times \mathbf{B})$ [15]. This force does not originate from Faraday effect. It is due to the phase slip that the vortex induces by moving from one point in the superconductor to another. Even though the mechanism that gives rise to the Nernst effect in a superconductor is different from that of a normal metal, Eq. 3 and Eq. 5 are still valid for superconductors since they are expressed in terms of general quantities such as $\bar{\sigma}$ and $\bar{\alpha}$. The only difference is that instead of electrons or holes, vortices should be thought of as the carriers of entropy, and the Josephson effect should be thought of instead of the Lorentz force.

Samples and Experimental Setup

The measurements were performed on $\text{Pr}_{2-x}\text{Ce}_x\text{CuO}_4$ ($x=0.13, 0.15, \text{ and } 0.17$) thin films grown by the pulsed laser deposition technique on STO substrates. The thickness of the

films was between 2000-3000 Å. The sample was attached on one end to a copper block with a mechanical clamp (for better thermal contact), with the other end left free (similar to a diving board-see Ref. [11] for a figure). A temperature gradient was created by heating up the free end with a small heater attached on the film. Two Lakeshore cernox thermometers were attached on the two ends of the sample to monitor the temperature gradient continuously. The temperature gradient was between 1-2.5 K/cm depending on the temperature of the measurement. The temperature of the sample was determined by taking the average of the temperatures at the hot and cold sides. The measurements were performed under vacuum, and the magnetic field was perpendicular to the ab-plane. The Nernst voltage was measured with a Keithley 2182 Nanovoltmeter which has a sensitivity of several nanovolts. The measurements were made at fixed temperatures while the field is scanned slowly at a rate of 20 Oe/sec. The temperature stability was a few millikelvins during the field scan. The Nernst signal is measured at positive and negative field polarity, and $(1/2)$ the difference of the two polarities is taken to remove any thermopower contribution.

Data and Analysis

Fig.1 shows the resistivity data for the films used in this study. The T_c , the sharpness of the superconducting transition, and the behavior of resistivity in high magnetic fields below the zero-field T_c (insulating-like for optimally-doped and under-doped samples, and metallic for over-doped samples) show the high quality of the films [11].

Fig.2-a, -b, -c show the low temperature Nernst effect data for the three dopings we studied, and Fig.2-d shows a comparison of the Nernst signal for the three dopings at $T/T_c \approx 0.7$. The superconducting vortex Nernst signal of the over-doped and optimally-doped samples crosses over to the normal-state Nernst signal (linear in magnetic field) very close to the resistive H_{c2} . In the under-doped sample, the transition from the superconducting state to normal state occurs over a wider field range suggesting that the fluctuation regime is broader for the under-doped regime compared to the other dopings. Nevertheless in all three dopings the Nernst signal behaves very differently from the hole-doped cuprates [1-4]. In the electron-doped PCCO the peak of the vortex Nernst signal is quite sharp in all the dopings

we studied. However, all the hole-doped compounds studied to date show an extended peak for the vortex Nernst signal that persists to fields much larger than the resistive H_{c2} even at temperatures very close to T_c .

Fig.3 shows that there is a clear distinction between the Nernst effect and resistivity for the under-doped sample (Fig.5b shows the similarity of Nernst effect and resistivity for the optimally-doped sample). The $T=9.7$ K Nernst effect data does not show the signature of the normal state (linear field dependence of the Nernst signal) up to 5-6 T, whereas the resistivity reaches the normal state value at 4 T. This behavior suggests that the Nernst effect is very sensitive to superconducting fluctuations which are difficult to observe in resistivity. Resistivity measurements on PCCO and NCCO have shown the H_{c2} of the under-doped compound to be smaller than that of the optimal-doped compound [16] (this can also be seen in the inset of Fig.1). This would imply that the magnitude of the superconducting gap is larger in the optimally-doped compound. However, point-contact tunnelling experiments on similar samples have shown that the superconducting gap amplitude is larger in the under-doped compound compared to the optimally-doped one [17]. Our Nernst effect data explains this contradiction by the insensitivity of the resistivity to superconducting fluctuations, and implies that resistivity is not a proper measurement for determining H_{c2} in agreement with the conclusion of Ref. [16].

Fig.4-a shows the typical Nernst effect for $T>T_c$ for the optimally-doped sample. The linear field dependence of the charge carrier Nernst effect is clearly seen, and no anomalous behavior is observed even at temperatures very close to the resistive T_c . Under-doped and over-doped samples behave very similarly to the optimally-doped sample, therefore the data for these dopings is not shown here. Fig.4-b summarizes the temperature dependence of the Nernst signal at 9 T for $T>T_c$. The dome-like behavior that was observed in $Nd_{1.85}Ce_{0.15}CuO_{4-\delta}$ for different oxygen dopings [11,12] is also observed in PCCO for different cerium dopings. The large magnitude of the Nernst signal is also similar to that observed in NCCO for $T>T_c$. This large magnitude of the Nernst signal and some other observations that are discussed in detail in Ref. [11] were interpreted as evidence for the existence of

two-types of carriers in electron-doped cuprates. In consistency with this previous interpretation, our present Nernst effect studies suggest that two-types of carriers exist in PCCO for all cerium dopings we studied. Quantitative analysis of how two types of carriers are introduced in the system, and the variation of their concentration with cerium and oxygen doping requires further systematic studies.

Whether the fluctuation region observed in the under-doped compound is related to the pseudogap state is an important issue. The experiments that studied the pseudogap state in electron-doped compounds have not yet produced conclusive results about either the magnitude or the onset temperature (T^*) of the pseudogap. The experiments in which evidence for the pseudogap state has been claimed are optical conductivity ($T^* > 292$ K [18] to $T^*=110$ K [19]), photoemission [20], Raman [21] ($T^*=220$ K), and tunnelling spectroscopy [17]. Unlike the experiments on hole-doped compounds that showed the pseudogap to be near the $(\pi, 0)$ region, the location of the pseudogap on the Fermi surface is also controversial for the electron-doped cuprates. Photoemission showed gap-like features near the intersection of the underlying Fermi surface with the antiferromagnetic Brillouin zone boundary whereas Raman spectroscopy showed a suppression of spectral weight for the B_{2g} Raman response in the vicinity of $(\pm\pi/2, \pm\pi/2)$.

Our Nernst effect data does not show a strong pseudogap related signal (e.g. vortex-like excitations or preformed pairs) in comparison with the hole-doped materials. For example, in the hole-doped compounds there is no distinctive feature in the Nernst signal when crossing T_c (i.e. T_c does not seem to be a special temperature). This would suggest that pseudogap related excitations dominate the signal around T_c . Our Nernst effect data shows a very different behavior around T_c , i.e. the distinctive vortex Nernst signal goes to a minimum and a clear normal state signal (linear in field) appears just above T_c (see Fig.2b for example). Therefore, we conclude that there is no strong pseudogap state related Nernst effect in this regime in the electron-doped superconductors. Quantitatively for the under-doped sample at $T \approx 15$ K, where an anomalous signal would be expected, the normal state contribution is around 100 nV/K, which is small compared to the vortex-like signal of several μ V/K around

T_c for under-doped $\text{La}_{2-x}\text{Sr}_x\text{CuO}_4$ [2]. However, we can not rule out the existence of a weak pseudogap signal that is dominated by the normal state (two-carrier) Nernst signal.

We now discuss the $H_{c2}(T)$ extracted from the Nernst signal (see Fig.5-a). The dashed lines in Fig.5-b show our method of extracting $H_{c2}(T)$. The uncertainty in the value of $H_{c2}(T)$ is found from the difference between the point of intersection of the dashed lines and the point one would get from extrapolating the vortex Nernst signal to zero. In our case extrapolating the vortex Nernst signal to zero is the same as extrapolating S_ϕ , the transport entropy per unit length of flux line, to zero since the flux flow resistivity is constant in the relevant field range ($S_\phi = \phi_o e_y / \rho_{ff}$, where ρ_{ff} is the flux flow resistivity and ϕ_o is flux quantum). Due to the complications of extracting the $H_{c2}(T)$ from S_ϕ that are detailed in Ref. [12] (usually $H_{c2}(T)$ is overestimated in this method), $H_{c2}(T)$ is not extracted from S_ϕ . In particular it was shown that determining $H_{c2}(T)$ from S_ϕ does not work at all for under-doped NCCO [12]. Therefore the errors in the value of $H_{c2}(T)$ are taken large enough to take into account this uncertainty. Considering the small difference between the $H_{c2}(T)$ values one would get by using different methods to determine it, some of the important results of this study would be valid in any of the methods used. One of these results is that $H_{c2}(0)$ increases with decreasing doping, since for a given T/T_c the signature of the normal state is seen at a larger field as the doping decreases. The other conclusion that would not change by the uncertainty in determining $H_{c2}(T)$ is that the fluctuation regime becomes narrower as the doping increases. This can be seen by comparing the close proximity of the vortex Nernst peak and the linear field dependent normal state contribution in the over-doped sample vs the broad transition region between these two typical regimes in the under-doped compound. However, one conclusion that would change for the under-doped compound is the linear temperature dependence of $H_{c2}(T)$. Using S_ϕ to determine $H_{c2}(T)$ would make it very difficult to observe any systematic temperature dependence for $H_{c2}(T)$ as was also found in Ref. [12].

The $H_{c2}(T)$ of the optimally-doped sample shows a linear temperature dependence in the range of our Nernst effect data. $H_{c2}(0)$ is estimated using the Helfand-Werthamer

formula [22]

$$H_{c2}(0) \approx 0.7 \times T_c \times \frac{dH_{c2}}{dT}, \quad (8)$$

where $\frac{dH_{c2}}{dT}$ is measured at T_c . $H_{c2}(0)$ for optimal doping is found to be 6.3 ± 0.2 T, and therefore the coherence length of the optimally-doped sample is $\xi(0) \approx 75 \pm 2 \text{ \AA}$ (from $\xi^2(0) = \frac{\phi_0}{2\pi H_{c2}(0)}$). The $H_{c2}(T)$ of the over-doped sample also shows a linear temperature dependence except for $T > 13$ K where the superconducting-to-normal state transition starts. Using the Helfand-Werthamer formula $H_{c2}(0)$ is found to be 3.7 ± 0.4 T, and $\xi(0) \approx 109 \pm 6 \text{ \AA}$. Due to the broad fluctuation region, where the Nernst signal had almost no field dependence, it was more difficult to determine $H_{c2}(T)$ for the under-doped sample. However, the fact that the normal state linear field dependence of the Nernst signal in the under-doped compound is observed at fields larger than that in the optimally-doped one suggests that $H_{c2}(T)$ is larger in the under-doped compound. A Helfand-Werthamer extrapolation to the $H_{c2}(T)$ vs T data for the under-doped compound yields $H_{c2}(0) = 7.1 \pm 0.5$ and $\xi(0) \approx 71 \pm 3 \text{ \AA}$. Resistivity and Nernst effect show similar $H_{c2}(T)$ for all dopings if the initial deviation from the normal state resistivity is chosen as a reference for $H_{c2}(T)$. The under-doped compound shows a larger difference between the Nernst effect and resistivity in terms of $H_{c2}(T)$, which suggests that the fluctuation regime is broader in the under-doped compound. A sample curve showing the superconducting-normal state transition from resistivity and Nernst effect is shown in Fig.5-b for the optimally-doped sample, and another curve is shown in Fig.3 for the under-doped sample.

There are important similarities between our Nernst effect data and the recent Nernst effect data on hole-doped Bi-2212 ($\text{Bi}_2\text{Sr}_2\text{CaCu}_2\text{O}_8$) and Bi-2201 ($\text{Bi}_2\text{Sr}_{2-y}\text{La}_y\text{CuO}_6$) [23]. Similar to our results, $H_{c2}(0)$ was found to increase with decreasing doping for both single layer and double layer Bi compounds studied in Ref[19]. These observations are consistent with other experiments showing an increasing superconducting gap ($\Delta_0 \propto v_f \sqrt{H_{c2}}$, where v_f is the Fermi velocity) amplitude with decreasing doping both for the n-doped and the p-doped cuprates [12,24].

Summary

Unlike in the hole-doped cuprates, the vortex Nernst signal in the electron-doped PCCO does not persist above T_c or H_{c2} for over and optimal dopings. The T_c or H_{c2} extracted from the Nernst measurements for these dopings are similar to those obtained from resistivity if the start of the resistive superconducting transition is chosen as a reference for T_c or $H_{c2}(T)$. The under-doped compound shows a broader fluctuation regime, and therefore the T_c and H_{c2} of this compound is different in Nernst effect and resistivity. Above T_c the temperature dependence of the Nernst voltage is very similar for different dopings, and the magnitude of the Nernst signal is too large to be explained by a one-carrier model. These results are consistent with our previous experiments on NCCO which were interpreted as evidence for the existence of a two-carrier transport in these materials [11].

The different behavior of the Nernst effect beyond the resistive T_c (or H_{c2}) for n-doped and p-doped cuprates in the optimal and over-doping is a puzzling problem that remains to be resolved. However, it is clear that the large Nernst signal seen in the normal state ($T > T_c$) of the n-doped cuprates has a different origin than the anomalous Nernst signal observed in the p-doped compounds. Why do we say this? In our data we see a clear distinction between the vortex Nernst effect contribution (a peak in the superconducting state) and the normal state contribution which is linear in magnetic field and which **increases** with temperature for $T > T_c$. In contrast, the anomalous Nernst signal observed in the p-doped compounds is not distinct (there is no feature at or around T_c that would distinguish the two contributions) from the vortex Nernst contribution, and the signal **decreases** with temperature for $T > T_c$ [2]. On the other hand, the larger coherence length and the much larger normal state Nernst effect of the n-doped compounds would make superconducting fluctuations smaller and less dominant in the n-doped cuprates close to T_c . Therefore, it is not possible to rule out the existence of a small vortex-like or preformed pairs contribution to the Nernst effect that is dominated by the large normal state Nernst signal.

In conclusion, we see several possible explanations that can reconcile the n-doped and p-doped Nernst experiments:

1) The large Nernst signal above T_c in the p-doped cuprates is caused by the superconducting fluctuations. Non-Gaussian fluctuations in addition to Aslamazov-Larkin Gaussian (non-interacting) fluctuations might be needed in order to explain the enhanced anomalous signal for the under-doped compound, but there is no need for vortex-like excitations above T_c . The effect of these fluctuations is smaller in the n-doped cuprates because the coherence length is much larger than in the p-doped materials.

2) The large signal for $T > T_c$ in p-doped cuprates is related to vortex excitations or other excitations associated with the pseudogap phase ($T^* > T > T_c$). These are not seen in n-doped cuprates because there is no pseudogap phase (or $T^* \leq T_c$). However, this explanation would contradict the existing experimental evidence for a pseudogap at high T^* in the n-doped materials.

3) The pseudogap does exist in the n-doped cuprates (and has $T^* \gg T_c$) but the contribution of the vortex-like excitations or preformed pairs to the Nernst effect can not be observed because of the larger two-carrier Nernst signal. However, as was mentioned in the discussion section, the magnitude of the anomalous Nernst signal observed in the p-doped cuprates around T_c is more than an order of magnitude larger than the normal state Nernst effect in n-doped cuprates around T_c . Therefore, unless the anomalous Nernst effect is very small (two-orders of magnitude less than that of the hole-doped cuprates), this explanation is not likely to be the reason for the difference between the n-doped and p-doped cuprates.

More work on the nature of the pseudogap state in the n-doped cuprates needs to be done before any conclusive explanation of the n-doped and p-doped Nernst effect data can be made. At the present time explanation (1) would appear to be most consistent with all the known experimental data.

This work was supported by the NSF DMR 01-02350.

REFERENCES

- [1] Z.A. Xu *et al.*, Nature **406**, 486 (2000)
- [2] Yayu Wang *et al.*, Phys. Rev. B **64**, 224519 (2001)
- [3] Yayu Wang *et al.*, Phys. Rev. Lett. **88**, 257003 (2002)
- [4] C. Capan *et al.*, Phys. Rev. Lett. **88**, 056601 (2002)
- [5] Tom Timusk and Bryan Statt, Rep. Prog. Phys. **62**, 61-122 (1999)
- [6] Hiroshi Kontani, Phys. Rev. Lett. **89**, 237003 (2002)
- [7] Iddo Ussishkin *et al.*, Phys. Rev. Lett. **89**, 287001 (2002)
- [8] Shina Tan and K.Levin cond-mat/0302248 v1 13 Feb 2003
- [9] S.J.Hagen *et al.* Phys. Rev. B **42**, 6777 (1990);
M. Zeh *et al.*, Phys. Rev. Lett. **64**, 3195 (1990);
H.-C.Ri *et al.*, Phys. Rev. B **50**, 3312 (1994)
- [10] X. Jiang *et al.*, Physica B, 194-196 (1994) 2305-2306
- [11] P. Fournier *et al.*, Phys. Rev. B **56**, 14149 (1997)
- [12] F. Gollnik and M. Naito, Phys. Rev. B **58**, 11734 (1998)
- [13] N.P.Armitage *et al.*, Phys. Lett. **86** 1126 (2001)
- [14] E.H. Sondheimer, Proc. R. Soc. London, Ser. A **193** 484 (1948)
- [15] B. Josephson, Phys. Lett. **16** 242 (1965)
- [16] P. Fournier and R.L.Greene, submitted to Phys. Rev. B and references therein.
- [17] A. Biswas *et al.*, Phys. Rev. Lett. **88**, 207004 (2002);
S. Kleefisch *et al.*, Phys. Rev. B **63**, R100507 (2001)
- [18] E.J.Singley *et al.*, Phys. Rev. B **64**, 224503 (2001)

- [19] C.C.Homes *et al.*, Phys. Rev. B **56**, 5525 (1997)
- [20] N.P.Armitage *et al.*, Phys. Lett. **87** 147003 (2001)
- [21] A. Koitzsch *et al.*, to be published in Phys. Rev. B
- [22] N.R.Werthamer *et al.*, Phys. Rev. **147**, 295 (1966)
E.Helfand and N.R.Werthamer Phys. Rev. **147**, 288 (1966)
- [23] Yayu Wang *et al.*, Science **299**, 86 (2003)
- [24] A.Ino *et al.*, Phys. Rev. B **65**,094504 (2002)

FIGURES

FIG. 1. Resistivity of the optimal, over, and under-doped PCCO as a function of temperature at zero field (dark symbols) and $H=14$ T (open symbols). The inset shows the resistivity of the same samples as a function of field at $T=2$ K.

FIG. 2. The low temperature Nernst effect of **(a)**-the under-doped, **(b)**-optimally-doped, **(c)**-over-doped samples as a function of magnetic field at fixed temperatures. Fig.2-**(d)** shows a comparison of the three dopings at roughly the same $T/T_c=0.7$.

FIG. 3. Comparison of resistivity ($T=10$ K) and Nernst effect ($T=9.7$ K) data for the under-doped sample.

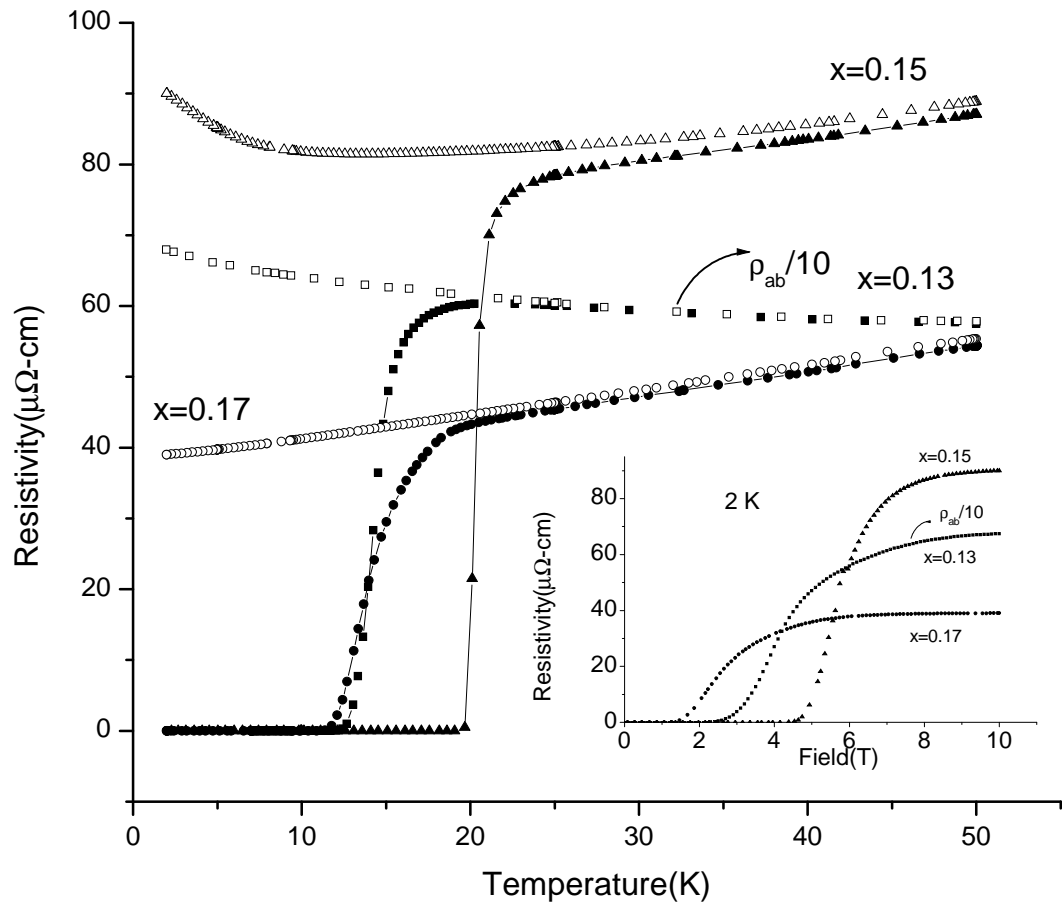
FIG. 4. **(a)**-High temperature Nernst effect as a function of magnetic field for the optimally-doped sample. **(b)**- The temperature dependence of the Nernst effect at $H=9$ T for all dopings.

FIG. 5. **(a)**-The upper critical field $H_{c2}(T)$ extracted from the Nernst effect data of Fig.2 (and other data omitted from Fig.2 for clarity). **(b)**-Comparison of Nernst effect and resistivity in terms of H_{c2} for $x=0.15$ sample. The dashed lines show the method used to extract H_{c2} .

TABLES

sample	resistive T_c	$H_{c2}(0)$	$\xi_0(0)$	dH_{c2}/dT
x=0.13	14 K	7.1 T	7.1 nm	0.41 T/K
x=0.15	20.5 K	6.3 T	7.5 nm	0.37 T/K
x=0.17	14.4 K	3.7 T	10.9 nm	0.35 T/K

TABLE I. Summary of our results.



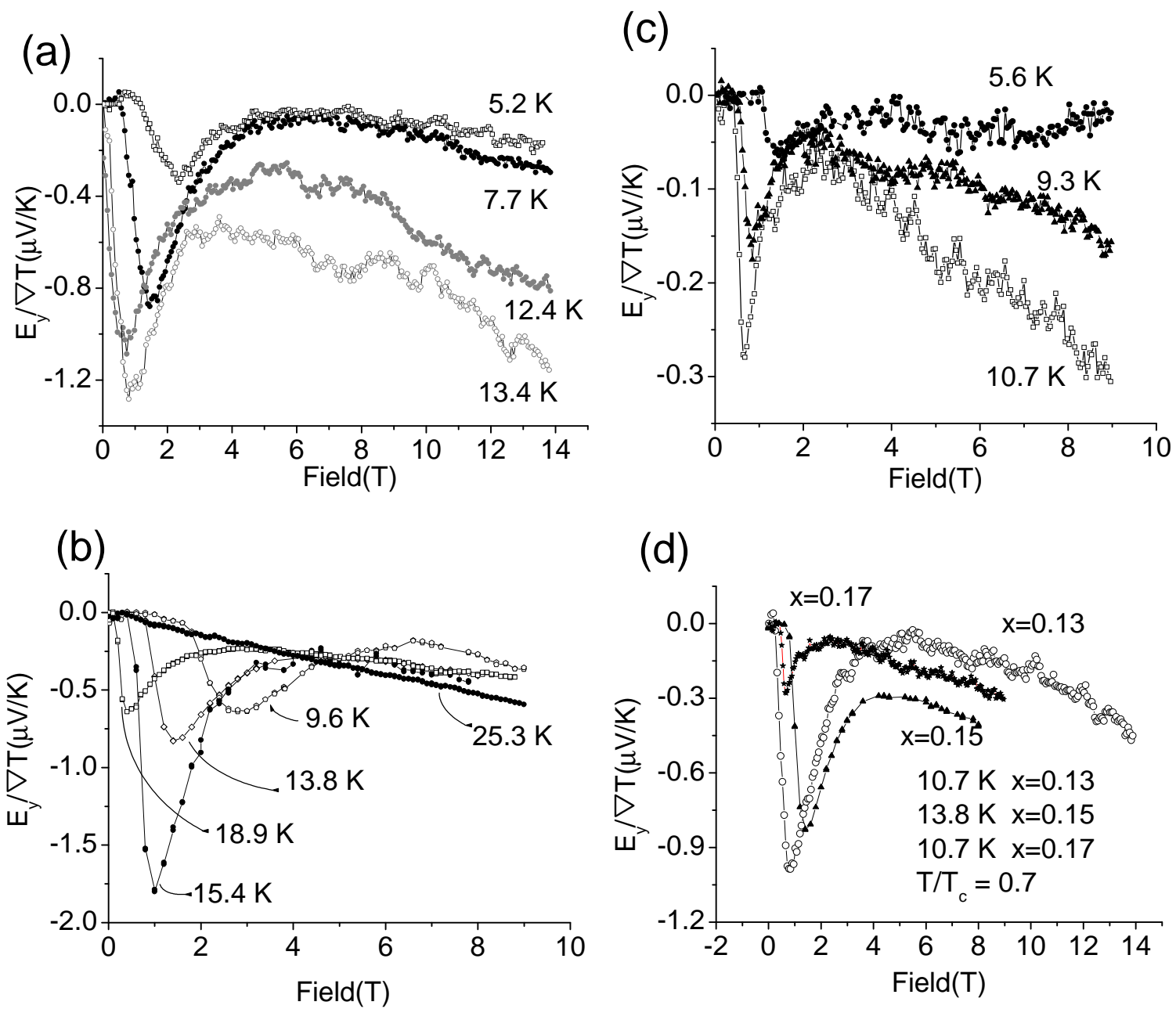


Fig. 2

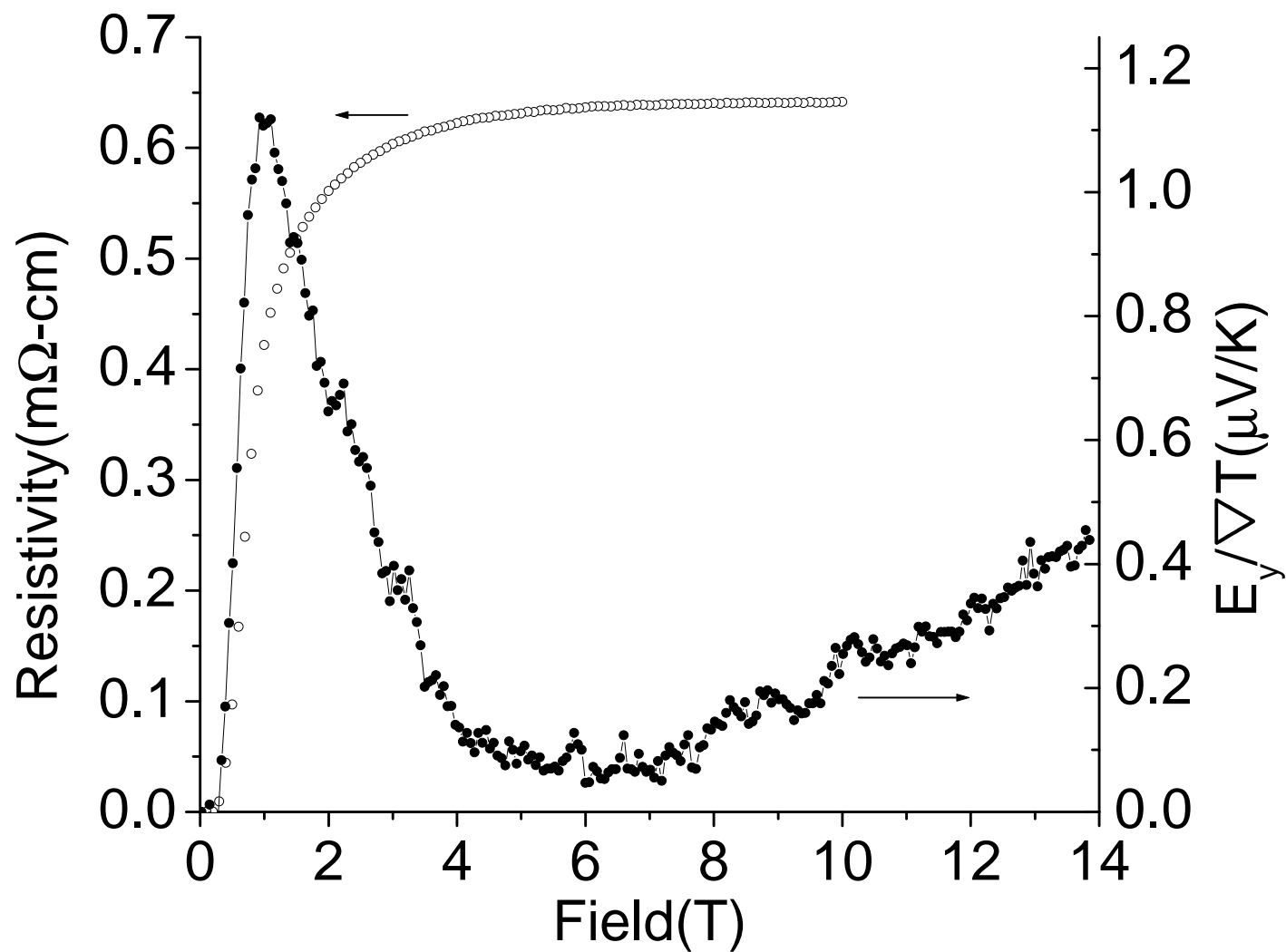


fig.3

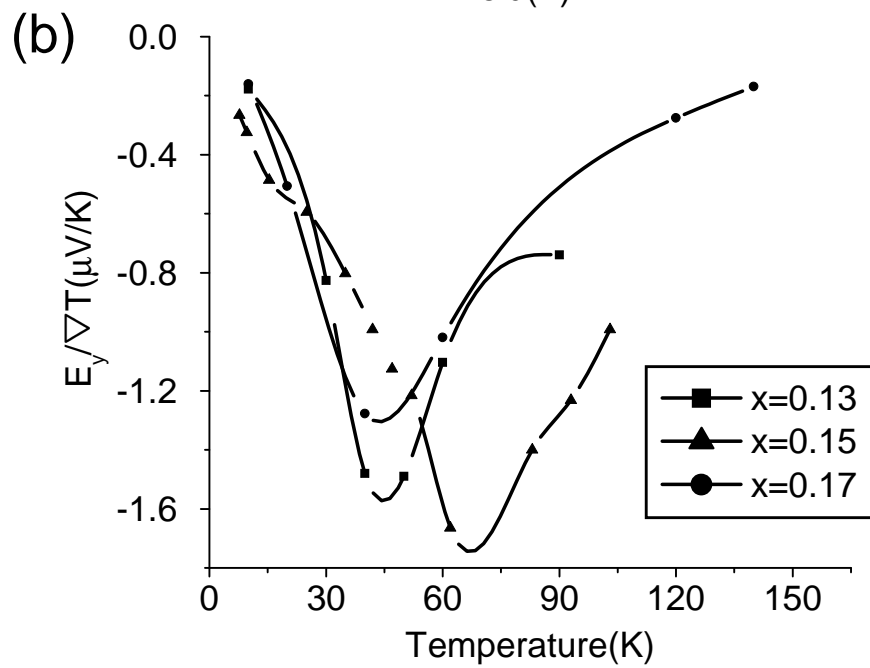
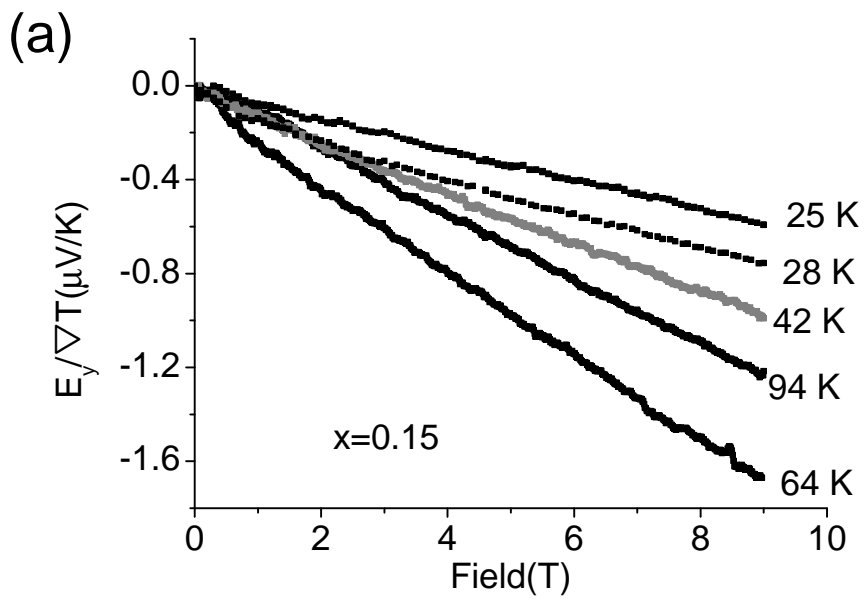


Fig 4

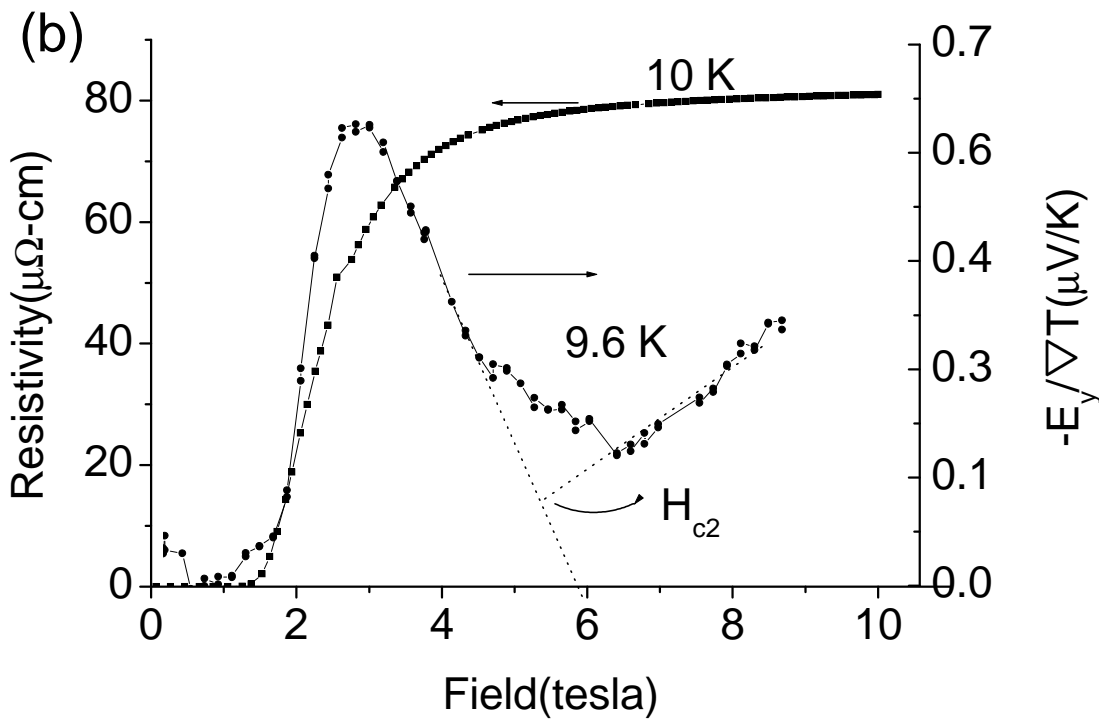
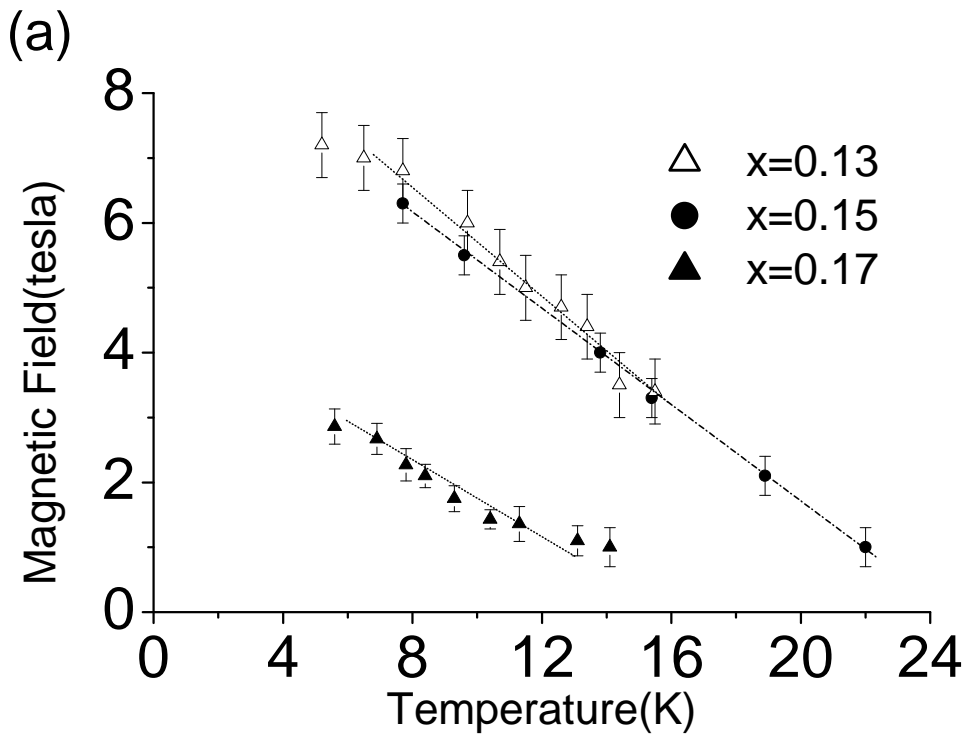


fig5